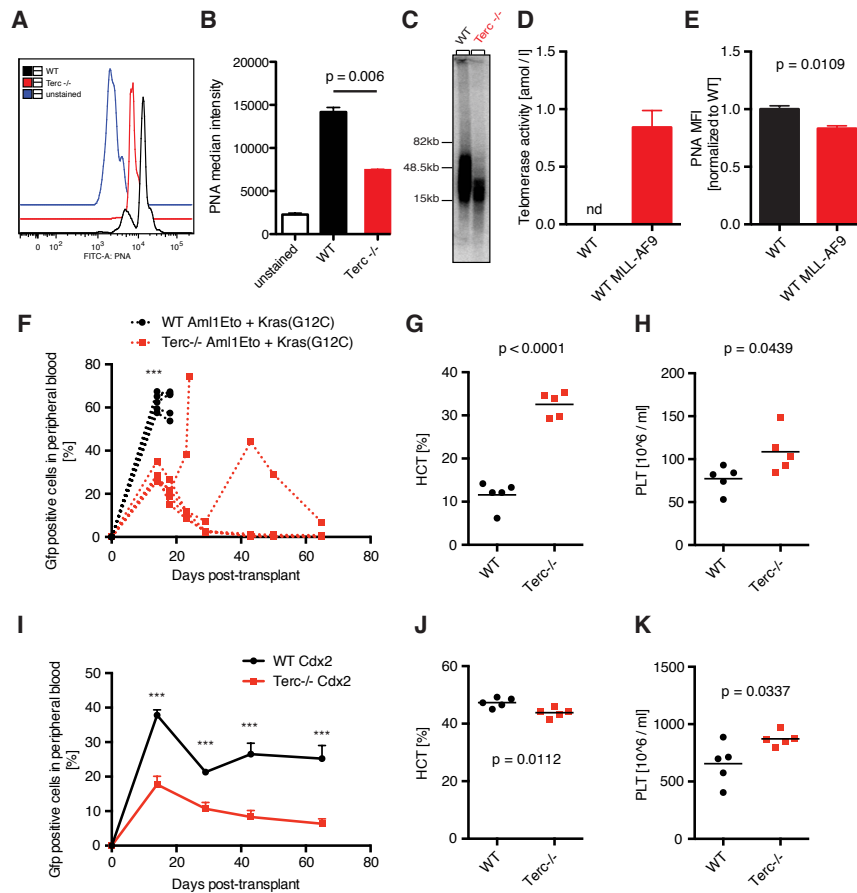


Figure S1

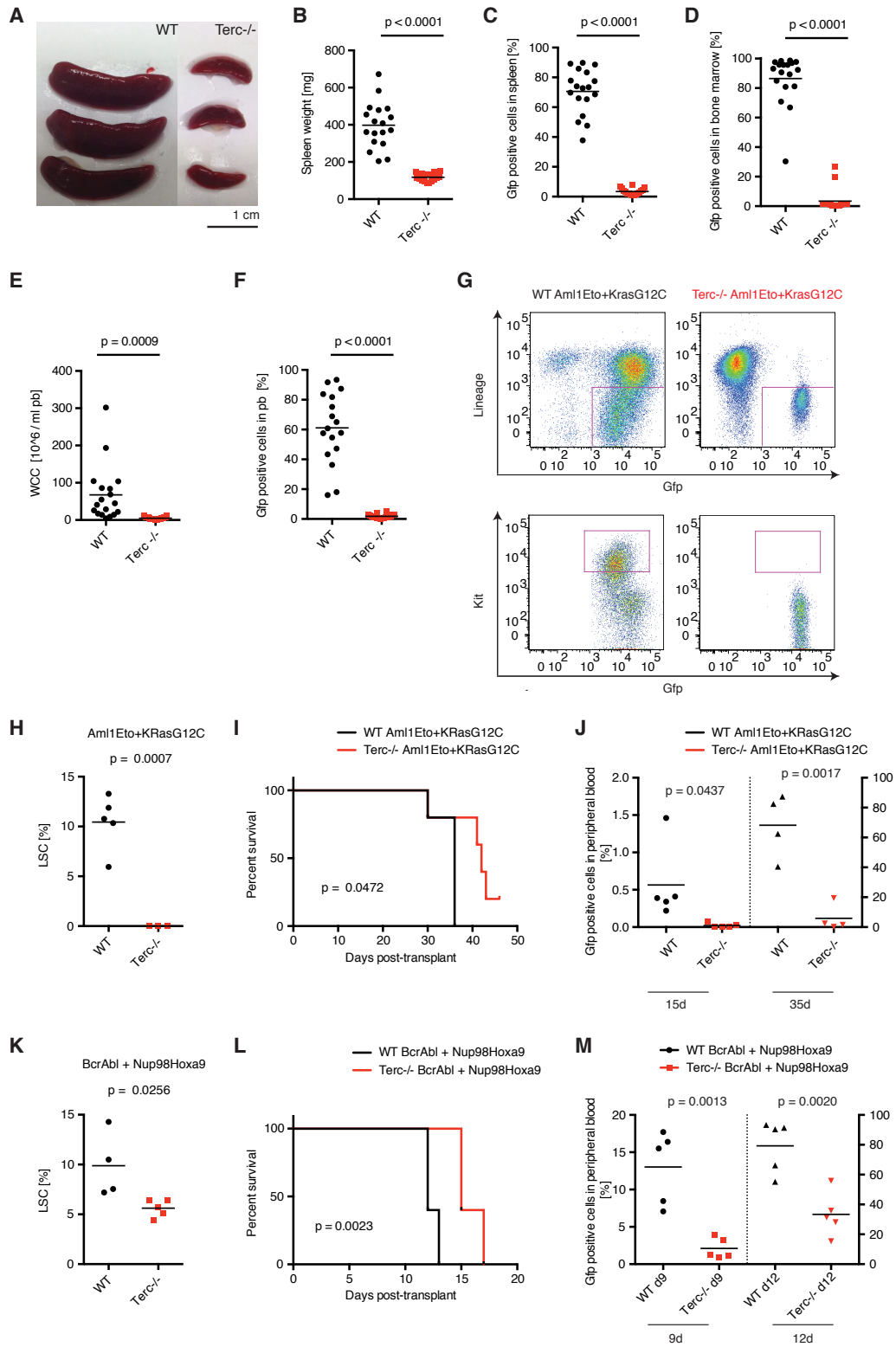


Supplementary Figure 1: Terc^{-/-} LSCs have shortened telomeres and delayed AML

onset *in vivo*. A) Flow cytometric analysis of telomere length using telomeric repeat - specific fluorescently labeled peptide nucleic acid (PNA). LKS⁺ were isolated from WT or Terc^{-/-} donors and transduced with MLL-AF9-neomycin resistance carrying retrovirus. Cells were plated into methylcellulose and passaged twice to deplete any non-transformed bone marrow. The graph displays PNA intensities of diploid WT MLL-AF9 LSC (black line), Terc^{-/-} MLL-AF9 LSC (red line) and unstained controls (blue line). B) PNA intensities are displayed as median \pm SE. Statistical significance was calculated based on Student's T test. N = 3. C) Telomeric restriction fragment analysis of WT MLL-AF9 and Terc^{-/-} MLL-AF9 LSCs. The image displays a radiograph from genomic DNA that was digested by restriction enzymes in the subtelomeric region, separated by pulse-field electrophoresis and subsequently labeled with telomeric repeat - specific radioactively labeled probes. D) Telomerase activity levels of viably sorted bone marrow cells from WT and MLL-AF9 primary recipients at disease onset. Mean \pm SE. N = 3. E) PNA fluorescent intensities in WT versus MLL-AF9 primary recipients at disease onset normalized to WT. Median \pm SE. N = 3. P = 0.0109 according to Student's T test. F) Levels of AML cells circulating in peripheral blood of primary recipients injected with WT or Terc^{-/-} Aml1Eto + Kras^{G12C} expressing lineage^{neg} bone marrow cells. G) Hematocrit (HCT) and H) platelet count in recipients of WT or Terc^{-/-} Aml1Eto + Kras^{G12C} AML at 18 days post-transplant. I) Engraftment of WT and Terc^{-/-} Cdx2-AML measured as circulating Gfp⁺ Cdx2-AML cells in the peripheral blood from primary recipients. J) Hematocrit (HCT) and K) platelet count in recipients of WT or Terc^{-/-} Cdx2-AML at 136 days post-transplant. N = 5. ***: p < 0.001 according to Student's T test.

Related to Figure 1.

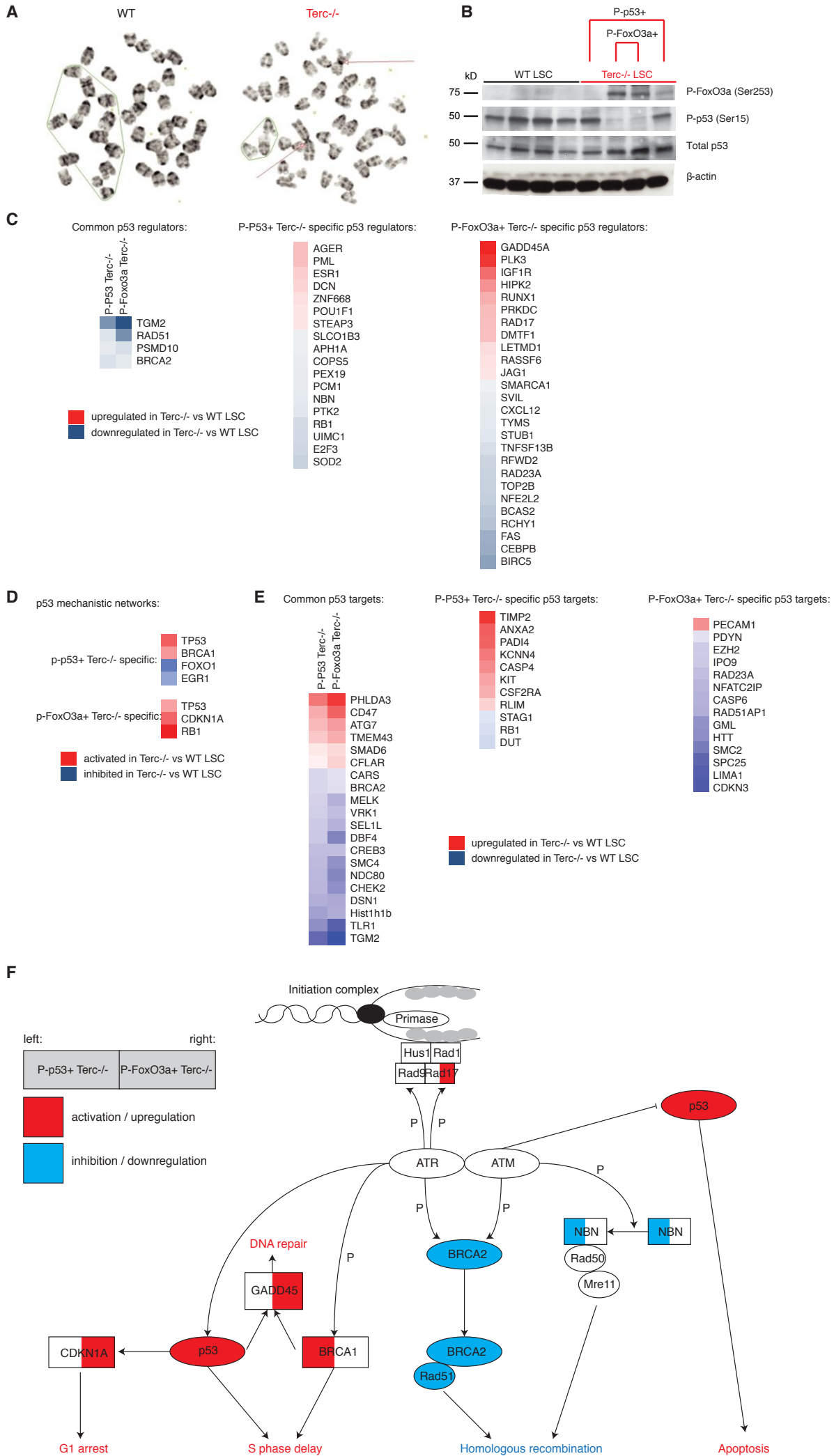
Figure S2



Supplementary Figure 2: Telomerase deficiency eradicates functional LSCs in murine MLL-AF9 AML. A) Spleen size, B) spleen weight, C) splenic AML cell infiltration, D) engraftment of AML cells in bone marrow, E) peripheral blood white cell counts, and F) levels of AML cells circulating in peripheral blood in secondary recipients injected with 20,000 viable WT or *Terc*^{-/-} AML cells from primary recipients at 28 days post-transplant. Photographs are representing the average spleen size from three independent experiments, and graphs display data from each individual animal from three independent experiments with each N = 6. Statistical significance was determined using Student's t test. G) Representative flow cytometry plots showing LSC populations from primary WT vs. *Terc*^{-/-} AML1ETO + KRAS^{G12C} AML mice at individual disease onset and H) quantification of LSCs. N = 3. I) Survival analysis and J) PB engraftment of secondary AML1ETO + KRAS^{G12C} AML recipients. N = 5. K) Quantification of LSCs in primary, L) survival analysis and M) PB engraftment of secondary WT and *Terc*^{-/-} BCRABL + NUP98HOXA9 AML recipients. N = 5. Median survival was 12 (WT) and 15 (*Terc*^{-/-}). P = 0.0023 according to Mantel-Cox test. All other statistical significance was calculated by Student's T-test.

Related to Figure 2.

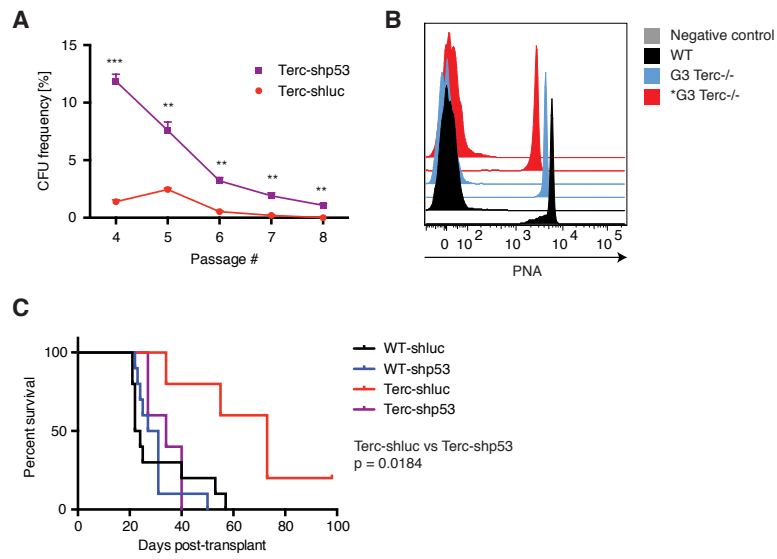
Figure S3



Supplementary Figure 3: Chromosomal instability and activated p53 signaling in telomerase-deficient LSCs. A) Example photographs of cytogenetic analysis of metaphase spreads from WT (left) and *Terc*^{-/-} (right) MLL-AF9 LSCs. B) Western blot analysis of phospho-FoxO3a (Ser253), phospho-p53 (Ser15), total p53 and beta-actin in WT and *Terc*^{-/-} LSCs sorted from primary recipients at disease onset. C) Heatmaps of differential transcriptional expression of upstream p53 regulators and E) downstream p53 targets in the identical *Terc*^{-/-} versus WT MLL-AF9 LSCs of primary recipients at disease onset as in Figure S3B divided into the two groups “p-p53+ *Terc*^{-/-}” and “p-FoxO3a+ *Terc*^{-/-}”. Upstream regulator analysis was carried out using Ingenuity Pathway analysis. D) Mechanistic networks for activated p53 and predicted activation states (below). Predicted activation (red) and inhibition (blue). F) Annotated ATR/ATM signaling with overlay of transcriptional up- (red) or downregulation (blue) in *Terc*^{-/-} vs WT MLL-AF9 LSC and predicted activation (red) or inhibition (blue) from upstream regulator analysis. The pathway illustration was adapted from Biocarta (www.biocarta.com).

Related to Figure 3.

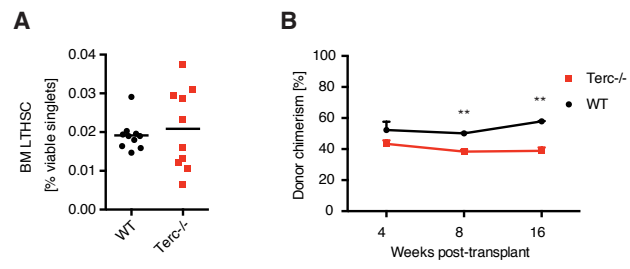
Figure S4



Supplementary Figure 4: Telomerase deficiency-mediated loss of LSCs is partially rescued by depletion of p53. A) WT MLL-AF9 and Terc^{-/-} MLL-AF9 LSCs were co-transduced with retrovirus carrying shRNA constructs targeting either p53 (shp53) or luciferase as negative control (shluc). Colony forming assay displaying the two conditions Terc-shluc (red) and Terc-shp53 (purple) during multiple passages as indicated on the x-axis. Colony forming units are displayed as number of colonies per input cells (%). Mean \pm SE. N = 3. B) Telomere length determined by PNA flow cytometry in splenic cells from WT (black) or two independent G3 Terc^{-/-} cohorts (blue / red). C) Survival analysis of secondary WT-shluc (black), WT-shp53 (blue), Terc-shluc (red) and Terc-shp53 (purple) MLL-AF9 LSC transplants. N = 5-10. Statistics was carried out using Mantel-Cox test. P = 0.0184 between Terc-shluc and Terc-shp53 groups.

Related to Figure 4.

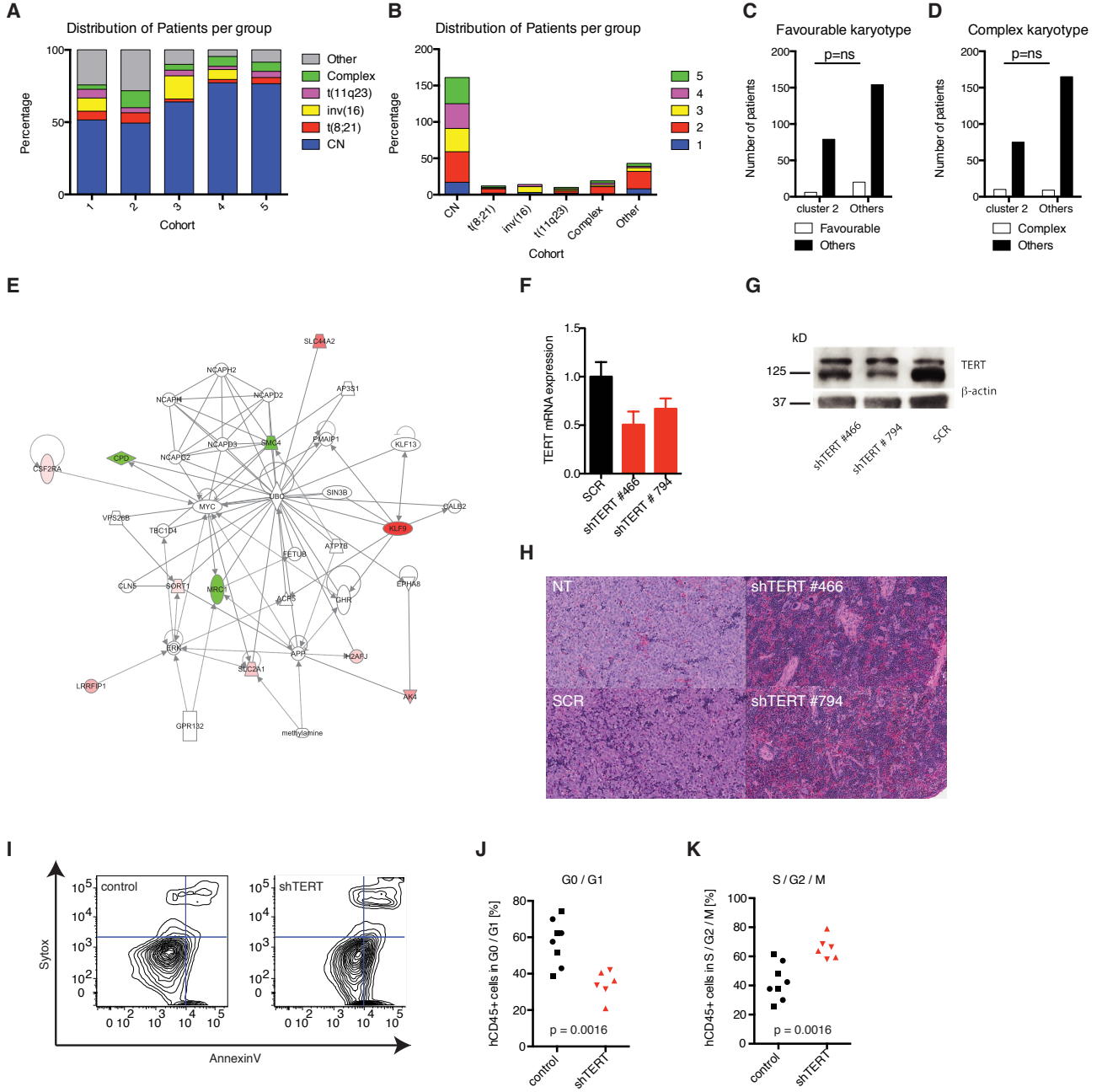
Figure S5



Supplementary Figure 5: Quantitative but stable reduction in normal HSC function upon telomerase loss. A) Quantification of WT (black) or *Terc*^{-/-} (red) bone marrow LT-HSC defined as lineage^{neg}, Kit^{high}, Sca1⁺, Cd150⁺, Cd48⁻. N = 5; the findings were confirmed in an additional independent experiment. B) Donor chimerism analysis in competitive *Terc*^{-/-} or WT LKS transplants. N = 5 (WT), N = 3 (*Terc*^{-/-}); Mean ± SE; **: p < 0.01; data were confirmed in an additional independent experiment.

Related to Figure 5.

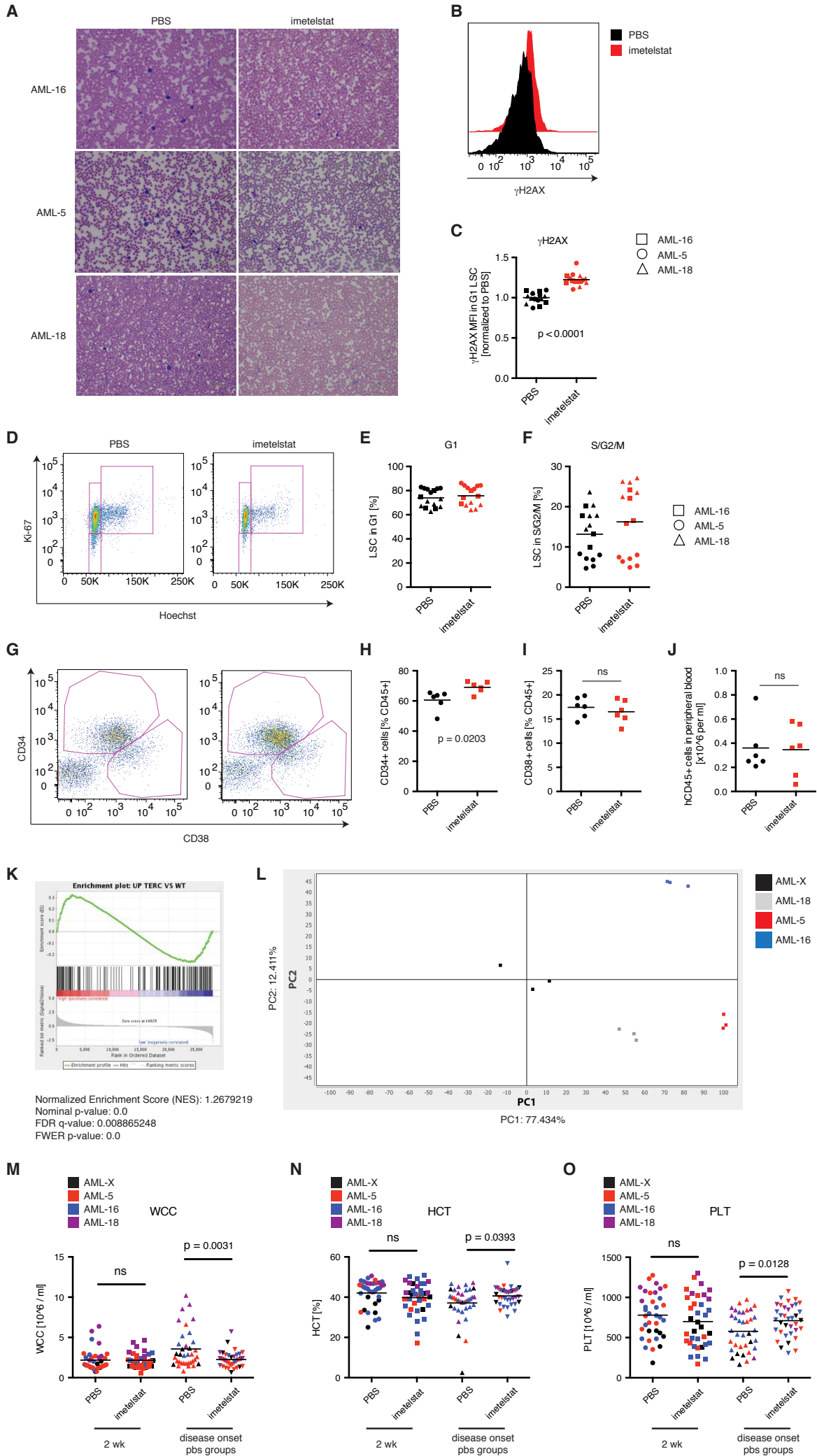
Figure S6



Supplementary Figure 6: Cytogenetics subtype analysis of the cohorts clustered according to the Terc signature in the Bullinger dataset. A) Distribution of patients per group as percentage; B) distribution of cohorts per cytogenetics subgroup; C) number of favorable and D) complex karyotype in the poor prognosis cluster 2 compared to all other clusters with improved prognosis. Statistical analysis was carried out using Chi-square test. E) Gene-gene interaction network generated by IPA on the short Terc^{-/-} signature identified by random forest modeling. F) mRNA expression and (G) protein expression analysis of TERT after shRNA knockdown vs. non-targeting control. Mean \pm SE from three biological replicates and confirmed in an additional independent experiment. H) Hematoxylin and Eosin staining of spleen sections from NT, SCR, shTERT#466 or shTERT#794 conditions at 47 days post-transplant. I) Example plots of apoptosis flow cytometry. Cell cycle analysis from hCD45⁺ populations three weeks post-transplant. Quantification of the distribution of Monomac6 in G0/G1 (J) and S/G2/M (K) cell cycle phases. Data were repeated in an additional independent experiment. Statistics were carried out using Student's T test.

Related to Figure 6.

Figure S7



Supplementary Figure 7: Pharmacological targeting of telomerase impairs human AML LSC function in primary AML xenografts. A) Wright-Giemsa staining of peripheral blood smears from PBS (left panels) or imetelstat (right panels) treated AML-16 (top row), AML-5 (middle row) or AML-18 (bottom row) xenografts. B) Example phospho-H2AX flow cytometry histogram and C) quantification of the median phospho-H2AX fluorescent intensities in G1 phase of CD45+ cells from AML-16 (squares), AML-18 (triangle), or CD34+CD45+ cells from AML-5 (circles) either treated with imetelstat (red) or vehicle control (black) normalized to controls. N = 6. $P < 0.0001$ according to Student's T test comparing the imetelstat-treated with the vehicle control treated groups. D) Example plot of cell cycle flow cytometry using Ki-67 to discriminate G0 from G1 and S/G2/M phases, and Hoechst to discriminate G0/G1 from S/G2/M cell cycle phases. Quantification of cells from CD45+ populations from AML-16 (squares), AML-18 (triangle), or CD34+CD45+ cells from AML-5 (circles) either treated with imetelstat (red) or vehicle control (black) in G1 (E) and S/G2/M phases (F). N = 6. Statistical significance was determined by Student's T test comparing imetelstat versus vehicle treated groups. G) Example plot of CD34/CD38 flow cytometry on splenic cells derived from AML-5:NSGS xenografts. Quantification of CD34+ (H) and CD38+ (I) populations. J) Secondary transplants of hCD45+ cells from imetelstat or vehicle treated primary AML-5:NSGS xenografts. Engraftment was measured by flow cytometry of hCD45+ cells circulating in the peripheral blood. K) Gene set enrichment analysis demonstrating enrichment of the upregulated *Terc*^{-/-} LSC signature in *Terc*^{-/-} vs WT LSC (human homologues of genes differentially expressed between *Terc*^{-/-} and WT LSC, $p < 0.01$) in AML-X compared to the other samples tested, q value < 0.01 , p value < 0.01 . L) Principal component analysis of the four AML patient samples according to the *Terc*^{-/-} LSC signature. No significant hematological toxicity of imetelstat-treated NSGS mice vs. vehicle controls showing M) PB WCC, N) hematocrit (HCT) and O) platelet counts after 2 weeks of treatment and just prior disease onset in the vehicle control groups (pooled data from 2 independent experiments per each AML genotype). Statistical significances were determined using Student's T test. Related to Figure 7.

Supplementary Table 1: Cytogenetic and molecular characterization of the patient derived xenograft samples.

Xenograft	FAB subtype	Cytogenetics	Known mutations and other notes
AML-5	M2	Monosomy 7	WT1 (SNP A->G at R16754)
AML-16	M4	Normal	FLT3-ITD+; NPM1+* (SNP G->T at W288C); IDH2* (SNP G->A at R140); WT1* (SNP A->G at R16754)
AML-18	M1	t(9;11), MLL translocation	KRAS (SNP G->C at G12D/V/A or G13D/A); WT1 (SNP A->G at R16754)
AML-X	M4	t(9;11), MLL translocation	

Supplementary Experimental Procedures

Telomere length and telomerase activity analyses

Viable cells were sorted (1×10^6 or 2×10^5 for telomere length and telomerase activity assays, respectively). Telomere length analysis was carried out using PNA kit/FITC for flow cytometry according to the manufacturer's instructions (Dako, Agilent Technologies), or by TRF analysis as described previously (Roberts et al., 2011). Telomerase activity levels were quantified using TeloTAGGG telomerase PCR ELISA kit (Roche) according to the manufacturer's recommendations.

AML retroviral bone marrow transplantation assays

Hematopoietic stem and progenitor populations were purified from bone marrow from WT or G3 Terc^{-/-} mice aged 6-12 weeks after red blood cell lysis (BD Pharmlyse, BD Biosciences) and stained with a lineage cocktail comprising of Cd3e (145-2C11), Cd5 (53-7.3), Ter119 (TER-119), Gr-1 (RB6-8C5), B220 (RA3-6B2) and Mac-1 (M1/70). Samples were lineage-depleted using biotin-binder Dynabeads (Invitrogen). The LKS⁺ populations were then transduced with MSCV-NUP98-HOXA9, MSCV-BCR-ABL, MSCV-AML1ETO, MSCV-KRas^{G12C} or MSCV-CDX2 containing retrovirus and transplanted into sublethally (5.5Gy) irradiated syngeneic WT recipients. The lateral tail vein was used for inoculation of leukemia cells. For serial transplantation assay, bone marrow or splenic GFP⁺ cells were harvested from primary recipients and injected into secondary sublethally irradiated syngeneic WT recipients. Mice were monitored for external (hunched posture, reduced movement, ruffled fur) and internal (i.e white blood cell counts) signs of leukemia.

Q-RT-PCR analysis

RNA was isolated using Qiagen RNeasy Mini extraction kit and reverse-transcribed into cDNA using Maxima H Minus First Strand cDNA synthesis kit (Thermo Scientific) according to the manufacturer's recommendations. Quantitative RT-PCR was carried out

using an ABI 7700 sequence detection system (Applied Biosystems, Foster City, CA). Reactions were performed in 20 ul volumes using SYBR Green PCR Master Mix (Applied Biosystems). Reaction mixes contained 8 ng cDNA. For the detection of human TERT transcripts relative to the housekeeping gene B2M, 6.25 pmol per reaction were used for each primer (TERT forward: 5'-CGGAAGAGTGTCTGGAGCA-3', and reverse: 5'GCACCCTCTTCAAGTGCTGT-3'; B2M forward: 5'- CTCGCGCTACTCTCTTTCT-3' and reverse: 5'- TCCATTCTTCAGTAAGTCAACT-3').

Western blotting

Cells were solubilized in Martins lysis buffer. Total protein concentrations were quantified using Biorad Protein Assay Dye Reagent Concentrate according to the manufacturer's recommendations. 25 ug of total protein extract were loaded on a 10% SDS-polyacrylamide gel (Mini-PROTEAN TGX gels; Bio-Rad Laboratories). After electrophoretic separation, samples were transferred to PVDF blotting membrane (Bio-Rad Laboratories). Unspecific binding sites were blocked in 5% BSA in TBS with 0.1% Tween for 1 h at 4C. Then, the membrane was incubated in primary antibody solution (primary antibody diluted in TBS-Tween and 5% BSA for over-night at 4C). The dilutions for rabbit anti-telomerase reverse transcriptase (Y182; Abcam), rabbit anti-phospho-FoxO3a (Ser253; #9466, Cell Signaling), rabbit anti-phospho-p53 (Ser15; #9284, Cell Signaling), and rabbit anti-p53 (ab131442, Abcam) were 1:1000. Mouse monoclonal antibody against beta-actin (AC-15; Abcam) was used as an internal calibrator in a dilution of 1:20000 and incubated for 30 min at room temperature. The membrane was washed 3 times in 0.1% (v/v) TBS-Tween and incubated with the secondary antibody (1:4,000 polyclonal goat anti-rabbit or anti-mouse immunoglobulin/HRP; Dako) in TBS with 0.1% TBS-Tween and 5% BSA for 1h at room temperature. The membrane was washed 6 times in 0.1% (v/v) TBS-Tween. Detection was carried out using Amersham ECL Western Blotting Analysis System according to the manufacturer's recommendations.

Cytogenetic analysis

Wild-type and telomerase-deficient cell lines were simultaneously cultured for 24 hr at 37°C in RPMI 1640 medium, supplemented with 20% fetal bovine serum.

Dividing cells were arrested by adding Demecolcine (SIGMA) for 10 minutes prior to harvesting. Cells were harvested as per standard procedure involving hypotonic treatment (0.075M KCl) and methanol/glacial acetic acid (3:1) fixation. Metaphase spreads were aged for 90 min at 90°C, followed by trypsin treatment and banding using Giemsa-Wright's stain. Images were captured on Leica Biosystems CytoVysion® station.

Gene expression profiling and bioinformatics analysis

Viable human AML patient cells (100,000; hCD45+ mCd45.1-) were purified from serially transplanted AML-X, AML-5, AML-16 and AML-18:NSGS xenografts in triplicate. RNA was extracted using Arcturus Picopure RNA isolation kit, pre-amplified using the Illumina Total Prep RNA amplification kit (Ambion) and hybridized on Illumina HumanHT-12 v4 expression BeadChip. The data were quantile-normalized with GenomeStudio (Illumina). The microarray dataset has been deposited in NCBI's Gene Expression Omnibus GEO Series accession number GSE63146 (<http://www.ncbi.nlm.nih.gov/geo/>). GSEA and principal component analysis of the *Terc*^{-/-} LSC signature containing the human homologues of both up- and downregulated genes in *Terc*^{-/-} vs WT LSCs ($p < 0.01$) on the human AML dataset was carried out using Genepattern (www.genepattern.broadinstitute.org). Upstream regulator analysis was carried out using Ingenuity pathway analysis. An upstream regulatory network of p53 was constructed based on literature-based evidence of direct or indirect interactions and overlaid with the observed gene expression changes in *Terc*^{-/-} vs WT LSCs using a cut-off of $p < 0.05$.

References

Roberts, A. R., Blewitt, M. E., Youngson, N. A., Whitelaw, E., and Chong, S. (2011). Reduced dosage of the modifiers of epigenetic reprogramming Dnmt1, Dnmt3L, SmcHD1 and Foxo3a has no detectable effect on mouse telomere length in vivo. *Chromosoma* 120, 377-385.